BIOCHEMISTRY
including biophysical chemistry & molecular biology
Article

Biochemistry **2009,** *48,* 7123–7131 7123
DOI: 10.1021/bi901015d

Properties of Arg481 Mutants of the aa_3-Type Cytochrome *c* Oxidase from *Rhodobacter sphaeroides* Suggest That neither R481 nor the Nearby D-Propionate of Heme a_3 Is Likely To Be the Proton Loading Site of the Proton Pump†

Hyun Ju Lee,‡ Linda Ojemyr,§ Ahmet Vakkasoglu,‡,∥ Peter Brzezinski,§ and Robert B. Gennis*,‡,∥

‡*Department of Biochemistry, University of Illinois, Urbana, Illinois 61801,* §*Department of Biochemistry and Biophysics, The Arrhenius Laboratories for Natural Sciences, Stockholm University, SE-106 91 Stockholm, Sweden, and* ∥*Center for Computational Biology and Biophysics, University of Illinois, Urbana, Illinois 61801*

Received June 16, 2009; Revised Manuscript Received June 30, 2009

ABSTRACT: Cytochrome *c* oxidase utilizes the energy from electron transfer and reduction of oxygen to water and pumps protons across the membrane, generating a proton motive force. A large body of biochemical work has shown that all the pumped protons enter the enzyme through the D-channel, which is apparent in X-ray structures as a chain of water molecules connecting D132 at the cytoplasmic surface of the enzyme to E286, near the enzyme active site. The exit pathway utilized by pumped protons beyond this point and leading to the bacterial periplasm is not known. Also not known is the proton loading site (or sites) which undergoes changes in pK_a in response to the chemistry at the enzyme active site and drives the proton pump mechanism. In this paper, we examine the role of R481, a highly conserved arginine that forms an ion pair with the D-propionate of heme a_3. The R481H, R481N, R481Q, and R481L mutants were examined. The R481H mutant oxidase is ~18% active and pumps protons with ~40% of the stoichiometry of the wild type. The R481N, R481Q, and R481L mutants each retain only ~5% of the steady-state activity, and this is shown to be due to inhibition of steps in the reaction of O_2 with the reduced enzyme. Neither the R481N mutant nor the R481Q mutant oxidases pump protons, but remarkably, the R481L mutant does pump protons with the same efficiency as the R481H mutant. Since the proton pump is clearly operating in the R481L mutant, these results rule out an essential role in the proton pump mechanism for R481 or its hydrogen bond partner, the D-propionate of heme a_3.

Cytochrome *c* oxidase is the terminal enzyme of the aerobic respiratory chains of most prokaryotes as well as all eukaryotic mitochondria. The enzyme couples the chemistry of reduction of O_2 (to $2H_2O$) to proton translocation across the membrane, generating a transmembrane electrochemical potential (*1*−*10*). The proton electrochemical gradient produced is then used to drive many energy-requiring processes, including the synthesis of ATP by the ATP synthase. A number of substantial questions about the mechanism of the proton pump remain to be answered, including identifying the exit pathway(s) of pumped protons and the site or sites which must bind and release protons during the catalytic cycle. Of particular interest in this work is the potential protonation site formed by the ion pair between a highly conserved arginine, R481 (in the *Rhodobacter sphaeroides* oxidase), and the D-propionate of heme a_3. This arginine/propionate ion pair has been thought to play critical roles in the exit pathways for both pumped protons and water (*11*−*15*).

In the *R. sphaeroides* and related oxidases, all of the pumped protons are transferred from the bacterial cytoplasm through the D-channel (*16*−*19*) to a highly conserved glutamate (E286) which is near the active site (Figure 1). From E286, the pumped protons are transferred to the exit channel and then to the bacterial periplasm. The question of the pathway used by pumped protons beyond E286 remains, although a number of studies have addressed this question (*12*, *15*, *20*−*27*). The proton pump requires at least one protonatable site which, during each electron transfer, binds a proton from the N-side of the membrane and then releases it to the P-side. Several candidates have been suggested as the "proton loading site" (*19*, *28*−*35*), including the A-propionate of heme a_3, W280, Cu_B ligands H333 and H334, and any of a cluster of interacting residues consisting of the D-propionate of heme a_3, R481, R482, and W172. The candidates that are closest to E286 are the D-propionate of heme a_3, along with R481 and W172, which each hydrogen bond to the D-propionate of heme a_3. The location of these residues, just "above" E286, has focused attention on these groups, either as the proton loading site or, at least, as water binding components within the exit pathway of pumped protons.

A set of mutations of R481 has been examined in the cytochrome bo_3 quinol oxidase from *Escherichia coli* (*12*, *36*). Puustinen and Wikström concluded (*12*) that proton pumping requires stabilization of the D-propionate of heme o_3 (equivalent to heme a_3) in the anionic state. The mutations of the *E. coli* oxidase indicate that although a positively charged side chain in the R481 position is not absolutely required for proton pumping, stabilization by hydrogen bonding of the deprotonated carboxylate of the D-propionate of heme o_3 is critical to pumping (*12*). The R481Q mutation is 70% active and pumps protons, whereas R481L (~40% active) did not pump protons.

†This work was supported by grants from the National Institutes of Health (HL16101 to R.B.G.), the Swedish Research Council (to P.B.), the Center for Biomembrane Research at Stockholm University (to P. B.), and the Knut and Alice Wallenberg Foundation (to P.B.).

*To whom correspondence should be addressed: Department of Biochemistry, A320 CLSL, MC-712, 600 S. Goodwin Ave., University of Illinois at Urbana−Champaign, Urbana, IL 61801. Telephone: (217) 333-9075. Fax: (217) 244-3186. E-mail: r-gennis@uiuc.edu.

Published on Web 07/04/2009

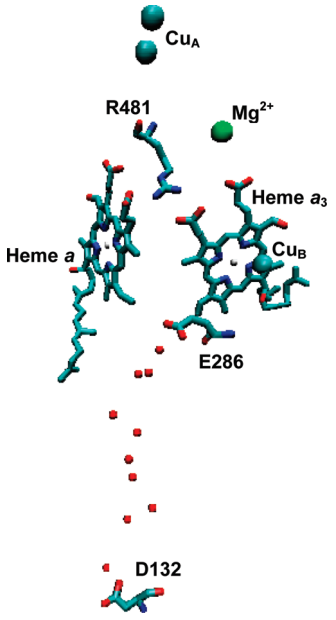

FIGURE 1: Structure of *R. sphaeroides* cytochrome *c* oxidase, defining the residues discussed. Of the three redox-active metal centers, heme *a* and the heme a_3−Cu_B binuclear center are in subunit I and Cu_A is in subunit II. The water molecules defining the D-channel used for the input of all the pumped protons from D132 to E286 are also shown. The figure was produced by using VMD starting from the crystal structure of Protein Data Bank entry 1M56 (*12*, *15*, *20*−*27*).

The main purpose of this work is to examine the equivalent mutations of R481 in the oxidase from *R. sphaeroides* to determine whether the previous conclusions can be universally applied. The results show that neither the positive charge at position 481 nor the capacity for hydrogen bonding to the adjacent D-propionate of heme a_3 is absolutely required for proton pumping. Neither R481 nor the D-propionate of heme a_3 is a viable candidate as the proton loading site in the mechanism of the proton pump.

MATERIALS AND METHODS

Mutagenesis. The Quik-Change mutagenesis kit from Stratagene was used to introduce the mutations. The PJS3-SH plasmid (*37*) was used as the template for the mutations, and then the pRK415-1 plasmid (*38*) was used as the expression plasmid. The expression plasmid with the mutation was transferred into S-17-1 cells by electroporation. The plasmid was transferred into the *R. sphaeroides* JS100 strain by conjugation. Restriction enzymes were from Invitrogen. Sequencing was performed by the University of Illinois Biotechnology Center.

Protein Purification. Cells were grown in Sistrom's minimal medium with 50 μg/mL spectinomycin, 50 μg/mL streptomycin, and 1 μg/mL tetracycline at 30 °C until the early stationary phase.

His-tagged wild-type and mutant enzymes were purified by histidine affinity chromatography. Cell pellets were homogenized in 50 mM potassium phosphate buffer (pH 6.5) with final concentrations of 1 mM EDTA,[1] 8 mM $MgSO_4$, DNase, and protease inhibitor cocktail. To break the cell, the suspended cell mixture was passed through a microfluidizer five times at a pressure of 20000 psi. Cell debris was spun down at 8000 rpm for 30 min, and the supernatant was ultracentrifuged at 40000 rpm for at least 5 h to pellet the cell membrane. The membrane was homogenized with 50 mM potassium phosphate buffer (pH 8.0) and solubilized with 2% (final concentration) dodecyl maltoside (DM), while being stirred for 2 h at 4 °C. The solubilized membrane was then ultracentrifuged at 40000 rpm for 1.5 h, and supernatant was added to the Ni-NTA resin and stirred for 2 h at 4 °C. The amount of Ni-NTA resin used was 1 mL of resin/mg of cytochrome oxidase estimated to bind (approximately 1 mg/L of growth medium). The resin with bound enzyme was loaded into the column. The column was washed until the flow-through was colorless, usually ~30 column volumes, with 50 mM potassium phosphate buffer (pH 8.0), 10 mM imidazole, and 0.1% DM. The oxidase was eluted with 50 mM potassium phosphate buffer (pH 8.0), 150 mM imidazole, and 0.1% DM. The enzyme was concentrated to ~20 mg/mL with a 50 kDa cutoff concentrator (Millipore), and the concentrated enzyme was desalted with a PD10 column (Amersham). The protein was aliquoted, fast-frozen in liquid nitrogen, and stored at −80 °C.

For the proton pumping assay, the enzyme was further purified by anion-exchange chromatography. The concentrated protein (5−10 mg) eluted from the Ni-NTA column was diluted at least 10-fold to a final volume of no more than 4 mL with buffer A [10 mM potassium phosphate buffer, 1 mM EDTA, and 0.2% DM (pH 7.2)] and loaded onto a tandem DEAE-5PW column (Toso-HaaS) attached to the FPLC system (Amersham, model AKTA Basic). The column was washed with buffer A and then eluted using a gradient with buffer B (buffer A with 1 M KCl). The enzyme eluted when the gradient was ~20% buffer B. The eluted protein was then concentrated, aliquoted, fast-frozen in liquid nitrogen, and stored at −80 °C.

UV−*Vis Spectroscopy*. A Shimadzu UV−vis-2101PC spectrophotometer was used to obtain the spectra of the enzyme (1.5 μM) in 50 mM potassium phosphate buffer (pH 8.0) and 0.1% DM. The concentration of the oxidase was determined from the dithionite reduced-minus-air-oxidized spectrum using the following relationships. The concentration of oxidase (millimolar) = $[A_{605}(\text{red-ox}) - A_{630}(\text{red-ox})]/24\ \text{mM}^{-1}\ \text{cm}^{-1}$, and the concentration of oxidase (millimolar) = $[A_{606}(\text{red}) - A_{640}(\text{red})]/40\ \text{mM}^{-1}\ \text{cm}^{-1}$.

Steady-State Activity Measurements. The steady-state activity of the enzyme was determined by the rate of oxygen consumption, monitored polarographically using a YSI model 53 oxygen meter equipped with a water-jacketed and stirred-glass measuring vessel. The reaction chamber was filled (1.8 mL) with 50 mM potassium phosphate buffer (pH 6.5), 0.1% DM, 10 mM ascorbate, 0.5 mM TMPD, and 30 μM horse heart cytochrome *c*. The enzyme was added to initiate the reaction.

Reconstitution of Oxidase into Phospholipid Vesicles. Cytochrome *c* oxidase vesicles (COVs) were used to measure the proton pumping stoichiometry (number of protons pumped per electron). Asolectin (soybean, 80 mg/mL), 2% cholic acid, and 100 mM HEPES-KOH (pH 7.4) were mixed and sonicated using a model W-375 sonicator (Heat Systems-Ultrasonics, Inc.). The solution was sonicated under a stream of argon gas for at least five cycles (until the sonicated mixture becomes clear), each cycle consisting of 1 min on followed by 1.5 min off. The oxidase was added to the sonicated lipid/cholate mixture to a final concentration of 0.9 μM. The detergent was slowly removed by the addition of aliquots of Bio-Beads (Bio-Rad). The Bio-Beads (66 mg/mL)

[1]Abbreviations: Ni-NTA, nickel nitrilotriacetic acid; DM, *n*-dodecyl β-D-maltoside; HEPES, 4-(2-hydroxyethyl)piperazine-1-ethanesulfonic acid; EDTA, ethylenediaminetetraacetic acid; TMPD, *N*,*N*,*N*′,*N*′-tetramethyl-*p*-phenylenediamine; RCR, respiratory control ratio; COVs, cytochrome oxidase vesicles; CCCP, carbonyl cyanide *p*-(trifluoromethoxy)phenylhydrazone; ATR, attenuated total reflectance; FTIR, Fourier transform infrared; NHE, normal hydrogen electrode.

were added every 30 min for 4 h at 4 °C. After this, the sample was diluted 1.5-fold with 100 mM HEPES-KOH buffer (pH 7.4). Additional Bio-Beads were added at room temperature: 133 mg/mL every 30 min for 2 h and, finally, 266 mg/mL every 30 min for 1 h. The solution was then dialyzed overnight against 60 mM KCl. These treatments result in the incorporation of the enzyme into small unilamellar vesicles. The lipid:protein ratio is selected to result in an average of fewer than one oxidase molecule per vesicle.

Proton Pumping Assay. Two different methods were employed to determine the stoichiometry of proton pumping, and both techniques yielded compatible results.

In the stirred-cell method, proton pumping is directly measured with a pH electrode. The stirred cell (1.5 mL) was filled at 25 °C with the enzyme solution, containing 60 mM KCl, 40 μM horse heart cytochrome *c*, 10 μM valinomycin, and 0.4 μM oxidase. Most of the O_2 was removed from this solution while it was being stirred under the stream of water-saturated argon gas. At this point, ascorbate was added to a final concentration of 300 μM. After equilibration, in which the final remnants of O_2 were removed by the oxidase, the reaction was initiated by injection of 10 μL of air-saturated water, equilibrated at 25 °C. The oxygen-saturated solution contains approximately 2.5 nmol of O_2, which is promptly consumed. Protons released or consumed are recorded by the pH electrode. After each determination, the system was calibrated by addition of 10 μL of an anaerobic 1 mM HCl solution (10 nmol of H^+).

Each of these experiments was repeated again in the presence of the protonophore CCCP (10 μM) to equilibrate the protons on the inside and outside of COVs. In all cases, the data indicated one proton was consumed per electron.

Proton pumping was also assessed using a pH-sensitive dye using a stopped-flow method (*39*) with an SX.17-MV model stopped-flow spectrophotometer from Applied Photophysics equipped with a diode array detector. Proton pumping of the COVs was measured by monitoring the absorption changes of phenol red at 557 nm, the isosbestic point of reduced and oxidized cytochrome *c* (*39*). Stopped-flow measurements were conducted by mixing a solution containing 60 mM KCl, 5 μM valinomycin, and 0.4 μM COVs (pH 7.4) with a solution containing 60 mM KCl, 10 μM reduced cytochrome *c*, and 40 μM phenol red (pH 7.4). The experiment was repeated with 10 μM CCCP added to the COV solution. Analysis of the data was conducted using the SPLINE function of MATLAB (The Mathworks, Inc.). Evaluation of the proton pumping was accomplished by comparing the proton consumption determined in the presence of CCCP to the proton release, determined in the absence of CCCP, but with valinomycin present to discharge any membrane potential.

Stopped-Flow Kinetics. The rate of reduction of the fully oxidized enzyme (reduction kinetics) was measured using the SX.17-MV model stopped-flow spectrophotometer from Applied Photophysics. The enzyme was freshly oxidized to avoid problems associated with the resting versus pulsed forms of the enzyme (*40*). A solution containing 50 mM Tricine (pH 8.0) and 0.1% DM with 5 μM oxidase was placed in the syringe barrel at the loading position of the stopped-flow system. Argon gas was applied to remove the oxygen in the syringe barrel. Ruthenium(III) hexamine (10 mM) and dithionite (30 mM) were added to fully reduce the enzyme. In the second syringe, air-saturated 50 mM Tricine (pH 8.0) and 0.1% DM were loaded. Once the contents had been mixed, the reaction of the reduced enzyme with O_2 was rapid, but the excess reductant present then re-reduced the enzyme. This re-reduction was monitored spectroscopically.

Preparation of Fully Reduced CO-Bound Cytochrome c Oxidase. The buffer was exchanged with 100 mM HEPES, 0.1% DM, and 50 μM EDTA (pH 7.5) using an Amicon Ultra instrument (Millipore, Billerica, MA). The sample with a final enzyme concentration of 5−10 μM was transferred to an anaerobic cuvette, and the atmosphere was exchanged to N_2 on a vacuum line. The anaerobic sample was reduced with 1−2 mM ascorbate and 0.5−1 μM ruthenium(III) hexamine. The atmosphere was then exchanged with CO.

Optical Flow-Flash Measurements. Fully reduced CO-bound oxidase, at a concentration of 5−10 μM in a buffer composed of 100 mM HEPES, 0.1% DM, and 50 μM EDTA (pH 7.5), was mixed in a 1:5 ratio in a modified stopped-flow apparatus (Applied Photophysics, Surrey, U.K.), with an O_2-saturated buffer of the same composition. Approximately 200 ms after the samples had been mixed, the CO ligand was dissociated by an 8 ns laser flash at 532 nm (Quantel, Brilliant B) and the enzyme reaction with O_2 was monitored optically as absorbance differences at single wavelengths. Data were analyzed using ProK (Applied Photophysics).

Electrochemistry. The FTIR difference spectra were recorded using the techniques previously described (*41*). A three-bounce attenuated total reflectance (ATR) attachment with a 3 mm diamond prism (SensIR now Smiths Detection) was used with a Bio-Rad (now Varian Inc.) FTS-575C FTIR spectrophotometer equipped with a liquid nitrogen-cooled MCT detector. A thin film containing the enzyme was adhered to the surface of the diamond prism. The initial step is to remove the detergent from the purified enzyme and pellet the enzyme. Ten microliters of a 150 μM enzyme solution was diluted 300-fold with water. The solution was concentrated using an Amicon 50 K membrane concentrator to a final volume of 500 μL. This dilution and concentration was repeated. The final suspension of enzyme was pelleted using a benchtop centrifuge. The pellet was resuspended in 10 μL of water and could be stored at −80 °C.

To prepare the protein film, 6 μL of this sample was pipetted onto the ATR diamond prism and air-dried for a few minutes. This caused the protein to stick firmly to the crystal surface. The presence of residual phospholipids in the preparation appears to help stabilize the enzyme and assist in the adherence to the surface. We rehydrated the protein film by first humidifying the air around the film until a stable FTIR spectrum was recorded. Then a 1 mL solution of the titration buffer [30 mM HEPES, 100 mM KCl, and 5 mM $MgCl_2$ (pH 7.5) in H_2O] was put on the film to rewet the sample. The protein concentration was estimated to be approximately 300 μM. The sample was sealed with an acrylic lid, designed to allow the space above the film to be perfused with a buffer of any composition. In this way, the redox status of the enzyme was altered, as previously described (*41*), to yield the fully reduced and fully oxidized states. When the buffer composition was changed, the state of the enzyme in the film was monitored by visible spectroscopy using a home-built apparatus with an Ocean Optics USB2000 spectrometer. The absorption spectrum in the visible range was obtained by reflectance off the surface of the sample on the diamond ATR crystal. Thus, one can record the visible spectrum simultaneously with the infrared spectrum as the applied potential is changed. In general, we equilibrated the sample with a buffer by passing the solution over the sample for ~2 h. A peristaltic pump (Cole-Parmer, Masterflex

C/L) was used for the flow of the buffer. All experiments were performed at 22 °C with a flow speed of 0.33 mL/min.

To achieve the electrochemical titration, a potentiostat (CV-27, BAS) was connected to the flow-electrochemical cell that was mounted on the ATR unit. The flow-electrochemical cell was designed as previously described (*41*), with gold particles (1−2 mm) as the working electrode and platinum-plated titanium electrode as the counter electrode. These two electrodes were separated by two ion-exchange membranes and a compartment that was filled with 400 mM phosphate buffer and continuously bubbled with argon gas to prevent any diffusion of oxygen into the titration buffer. Three mediators were used to equilibrate the potential of the protein film with the titration buffer: potassium ferrocyanide (420 mV vs NHE), ruthenium(III) hexamine (50 mV vs NHE), and menadione (−12 mV vs NHE). A Ag/AgCl reference electrode was located on the ATR unit close to the protein film.

Titrations were repeated with at least two different sample films. Each high-potential step was followed by equilibration at −292 mV (vs NHE) to record a background and also reduce any oxygen that might have leaked into the sample compartment. Equilibration times for each point were ~30 min.

Since there are four redox-active centers in the enzyme, a quantitative fit to the data was not attempted. The results were analyzed qualitatively to observe whether the mutations influenced the electrochemical properties of the hemes.

RESULTS

The following mutants were made: R481H, R481N, R481Q, and R481L. Each mutant oxidase was purified to homogeneity and characterized.

UV−Vis Spectra. The wild-type aa_3-type oxidase from *R. sphaeroides* has a characteristic absorption spectrum with a Soret band at 424 nm and an α band at 600 nm in the oxidized state. Upon reduction via addition of dithionite, the Soret band and α band shift to 445 and 605 nm, respectively. The Soret band at 445 nm is contributed by both low-spin heme *a* and high-spin heme a_3. In the α band, heme *a* mainly contributes up to 80% of the peak (*42*).

In spectra of the dithionite-reduced enzymes, both the Soret band and α band are shifted for all of the mutants. In R481H, the absorption peaks are shifted to 442 and 603 nm, respectively, and for the rest of the mutants, the two peaks are shifted slightly more, to 441 and 602 nm for the Soret band and α band, respectively (Figure 2). In other words, the data indicate that the environments of heme *a* and heme a_3 are perturbed by all of the R481 mutations.

Steady-State Activity. All the mutants exhibit steady-state activity lower than that of the wild-type oxidase (Table 1). R481H, which can maintain a salt bridge and hydrogen bond to the carboxyl of the D-propionate, has 18% of the oxidase activity. R481N, R481Q, and R481L each have ~5% of the wild-type oxidase activity. These values compare to the activity of the equivalent mutations in the *E. coli* bo_3-type quinol oxidase (*12*): R481N (~60%), R481Q (~50%), and R481L (~40%).

Electrochemical Titrations. Electrochemical titrations of the wild-type oxidase were conducted using the enzyme deposited as a thin film on a diamond ATR, perfused with buffer at pH 7.5 (Figure 3). The titrations were conducted by monitoring the absorbance at 602 nm and varying the electrochemical solution potential using a potentiostat. The data could be roughly viewed as exhibiting two redox steps with a high-potential step at 452 mV (vs NHE) and a low-potential step at 136 mV (vs NHE). FTIR difference spectra, recorded simultaneously (not shown), displayed the same two steps and confirmed that each of the two steps contains contributions from both heme *a* and heme a_3.

The same two-step titration is observed with the R481L mutant, but with the midpoints shifted to 419 mV (vs NHE) and 78 mV (vs NHE). The shape of the redox titration curve for the wave at 78 mV is steeper than that of the equivalent redox process with the wild-type oxidase, suggesting cooperativity. However, this is an artifact due to incomplete equilibration with

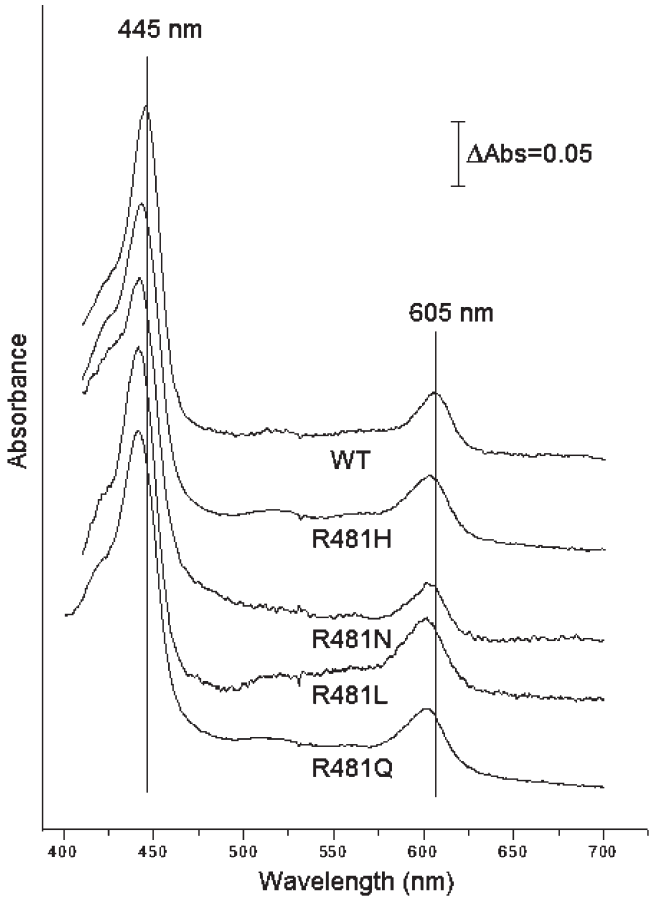

FIGURE 2: UV−visible spectra of the dithionite-reduced oxidases: wild type, R481H, R481N, R481L, and R481Q. Both the Soret band at 445 nm and the α band at 605 nm are shifted in all of the mutants.

Table 1: Comparison of Activities of Wild-Type and Mutant Oxidases from *R. sphaeroides* before and after Reconstitution

	activity ($e^- s^{-1} aa_3^{-1}$)			
		in vesicles		
oxidase	in detergent	controlled[a]	uncontrolled[b]	RCR[c]
wild type	1100	32	312	10
R481H	201	17	150	9
R481L	54	25	96	4
R481N	63	25	71	3
R481Q	43	14	57	4

[a] Measured in the absence of ionophores. [b] Measured in the presence of the protonophore CCCP. [c] The ratio of the uncontrolled to controlled enzyme turnover numbers.

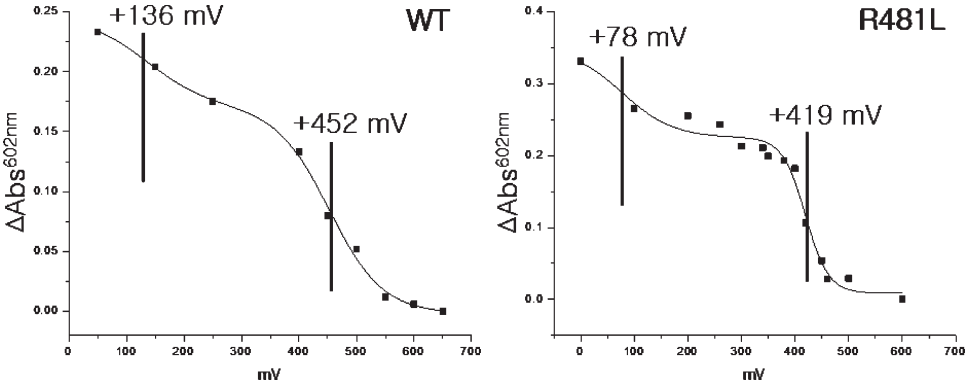

FIGURE 3: Electrochemical titrations of the *R. sphaeroides* wild-type and R481L mutant oxidases. The solution potential (vs NHE) is plotted vs the absorbance at 602 nm. The lines are simply a polynomial fit and not based on any model. The estimated midpoints of the two waves are indicated. The midpoints are shifted to lower values in the R481L mutant. The steep curve for the titration of the R481L mutant is due to incomplete equilibration, so the value of the midpoint (419 mV) should be considered to be an estimate.

the mutant. The data should not be considered quantitatively, therefore, but the trend is clear. The leucine substitution for arginine results in destabilization of the reduced form of the hemes, reducing the midpoint potentials by ~35 and ~60 mV for the high- and low-potential steps, respectively. The shifts are in the expected direction based on removal of a positive charge from the vicinity of the hemes.

Respiratory Control and Proton Pumping. To assess proton pumping of the isolated enzymes, both wild-type and mutant enzymes were reconstituted in the vesicles. The extent to which the vesicles are able to maintain a proton motive force is indicated by the respiratory control ratio (RCR). This is the ratio of the steady-state oxidase activity of the vesicle-reconstituted enzyme in the presence of uncoupler (uncontrolled activity) to the activity in the absence of uncoupler (controlled activity). The controlled oxidase activity is limited if a proton motive force is generated across the vesicle membrane, and this activity is increased upon addition of CCCP (protonophore) and valinomycin (ionophore), which collapse the proton electrochemical gradient. Each of the mutant enzymes exhibits an RCR substantially greater than 1 (Table 1), indicating that each enzyme is generating a proton motive force.

The proton pumping assay was performed using the stir-cell method with a pH-sensitive electrode and stopped-flow method using the enzyme-reconstituted vesicles. Data are shown only for the stopped-flow method (Figure 4), but the results of both methods are essentially the same.

Using a stopped-flow method, the pH changes in solution were monitored with a pH-sensitive dye. After the solutions containing the enzyme and excess oxygen were mixed, the reaction that ensued was limited by the amount of reduced cytochrome *c* present. The data from the stopped flow definitively show that the wild type pumps protons (Figure 4A) and that R481L (Figure 4B) also pumps protons but with a lower stoichiometry. There is no indication of proton pumping by R481Q (Figure 4C) or by R481N (not shown). R481H pumps protons with approximately the same stoichiometry as does R481L (not shown). In all cases, in the presence of the protonophore CCCP, net alkalinization was observed due to proton consumption from the reduction of oxygen to water. Note that for the wild-type enzyme, the rate of alkalinization is considerably faster than the rate of proton pumping (Figure 4A). This reflects the fact that in the presence of the uncoupler, the enzyme specific activity increases 10-fold (see Table 1).

Stopped-Flow Reduction Kinetics. To determine the extent to which the mutations in R481 alter the rate of reduction of the fully oxidized enzyme, a stopped-flow spectrophotometer was used. The fully oxidized enzyme was mixed with ruthenium(III) hexamine. The reduction rate of the hemes (not resolved into heme *a* and heme a_3) was monitored using the Soret band at 445 nm. The wild type and R481H mutants are reduced by ruthenium(III) hexamine at approximately equal rates (~160 s^{-1}), and the greatest influence on the rate of reduction, observed for the R481Q mutant, is slower by a factor of only 2 (~80 s^{-1}) (Table 2).

Flow-Flash Measurement of the Oxidation of the Fully Reduced Enzyme. To determine how the R481 mutants slow the rate of oxidation of the fully reduced enzyme, the flow-flash assay was utilized to compare the wild-type enzyme with the R481H, R481Q, and R481L mutants. In this assay, the reaction is initiated by photolysis of the CO adduct of the fully reduced enzyme in the presence of O_2. Since the reaction is not rate-limited by the process of mixing solutions, fast processes can be time-resolved. Earlier experiments with the wild-type enzyme showed that there are four sequential steps (*43*) (Table 3): (1) R→A, formation of the initial complex of the reduced enzyme with O_2; (2) A→P_R, reaction splitting the O−O bond to form the oxoferryl form of heme a_3 with the concomitant oxidation of heme *a*, but without the transfer of a proton to the active site; (3) P_R → F, transfer of a proton from E286 to the active site, converting $^-$OH to H_2O associated with Cu_B(II); and (4) F→O, coupled electron transfer from heme *a* and proton transfer from E286 to the active site. The two latter reactions are linked to proton pumping (*44*, *45*). The reaction of fully reduced R481H with O_2 is nearly the same as that of the wild-type oxidase, except that the F → O step is slowed by ~4-fold (Figure 5 and Table 3). This correlates with the 18% steady-state turnover of the R481H mutant.

The reaction of fully reduced R481Q with O_2 is much more perturbed (Figure 5 and Table 3). The initial combination of O_2 with heme a_3 proceeds at the same rate as that of the wild type, indicating that the structure of the active site and pathway for O_2 are not altered. The rate of the A→P_R step is slowed by ~6-fold. The steps following it, P_R→F and F→O, are not clearly resolved in part because of the spectroscopic changes due to the mutation. However, it is estimated that the rate of the P_R → F step is ~100-fold slower than that of the wild type. The reaction to form the O state may not be complete on the 1 s time scale. These data

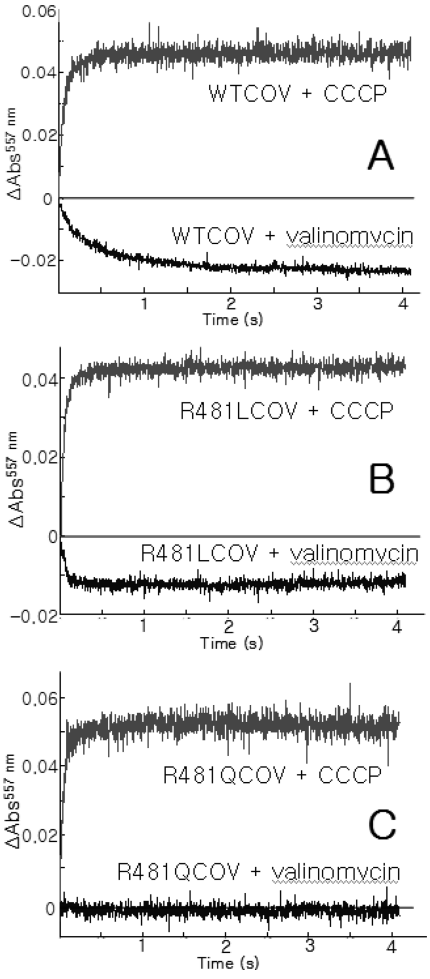

FIGURE 4: Proton pumping determined by monitoring the absorbance change of phenol red at 557 nm using a stopped-flow spectrophotometer. An absorbance increase indicates alkalinization, which is observed in the presence of the protonophore CCCP. In the presence of valinomycin, without CCCP, the change in the phenol red absorbance is downward, indicating acidification due to proton pumping for both (A) the wild-type oxidase and (B) the R481L mutant. In contrast, the acidification is not observed with (C) the R481Q mutant oxidase. If the alkalinization is thought to be due to the consumption of one proton per electron, the amplitude of the absorbance change in the presence of CCCP can be used to estimate the stoichiometry of proton release, assuming that the buffering capacity before and after addition of the uncoupler remains constant. For the wild-type enzyme (A), the rate of enzyme turnover is ~10-fold larger for the decoupled enzyme in the presence of CCCP than in the absence of the uncoupler. For this reason, the rate of alkalinization is substantially faster than the rate of proton pumping, which is measured with the coupled enzyme.

Table 2: Rate Constants for Reduction of the Wild-Type and Mutant Oxidases by Ruthenium(III) Hexamine

oxidase	k_{red} (s^{-1})
wild type	156
R481H	160
R481L	98
R481N	136
R481Q	82

indicated substantial perturbation, perhaps due to slow transfer of a proton to the active site that is required for both the $P_R \rightarrow F$ and $F \rightarrow O$ steps of the reaction. This mutant does not pump protons.

Table 3: Time Constants ($\tau = 1/k$) for the Four Steps Time-Resolved for the Reaction of the Fully Reduced Oxidase with O_2

	τ (μs)			
oxidase	R→A	A→P	P→F	F→O
wild type[a]	8	40	0.1	1.1
R481H	6	40	0.1	3.7
R481L	26	1000	10[b]	10[b]
R481Q	9	250	10	10

[a] Data for the wild type are from ref *43*. [b] Not resolved. Assumed to correspond to the F → O transition.

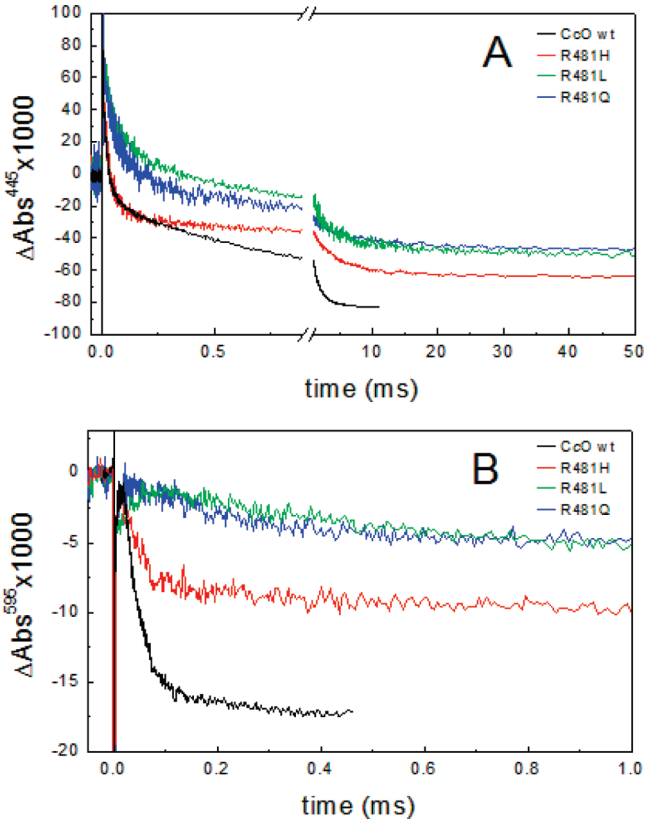

FIGURE 5: Flow-flash reaction of fully reduced wild-type, R481H, R481Q, and R481L oxidases. (A) The reaction was monitored at 445 nm. (B) The reaction was monitored at 595 nm. Experimental conditions: 5−10 μM fully reduced and CO-bound oxidase mixed in a 1:5 ratio with an oxygen-saturated buffer containing 100 mM HEPES, 0.1% DM, and 50 μM EDTA (pH 7.5). Traces are scaled to 1 μM reacting enzyme.

The most interesting mutant, R481L, displays even greater indications of perturbation (Figure 5 and Table 3). The rate of binding of O_2 is ~3-fold slower, likely a perturbation to the structure of the active site or of the normal pathway used by O_2 to reach heme a_3. The rate of the $A \rightarrow P_R$ step is substantially slower than that of the wild type (25-fold), indicating a slower rate of transfer of an electron from heme *a* to the active site. As with the R481Q mutant, the steps following the formation of the P_R state are not clearly resolved, though it is evident that there is a very large decrease in the rates of these steps. Most remarkably, despite the large perturbations evident from the R481L mutation, the mutant oxidase still pumps protons.

DISCUSSION

The motivation for this work was to test the importance of the ion pair of R481 and the D-propionate of heme a_3 in the mechanism of the proton pump of the heme copper oxidases. Previous work (*12*) on the cytochrome bo_3 quinol oxidase from *E. coli* indicated that proton pumping requires stabilization of the anionic form of the carboxylate of the D-propionate of heme a_3. Most notably, with the *E. coli* oxidase, R481Q (60% active after isolation), which can form a hydrogen bond to the D-propionate, can pump protons, whereas R481L (40% active after purification), which cannot form a hydrogen bond to the D-propionate, does not pump protons. The most important result from this work is that the R481L mutant oxidase from the aa_3-type oxidase from *R. sphaeroides* can pump protons. This result virtually rules out R481 as well as the associated D-propionate of heme a_3 as being the proton loading site in the proton pump mechanism. Assuming a common mechanism, this conclusion should apply generally to all the proton-pumping heme copper oxidases.

Previously, the R481K mutant has been characterized in both the *R. sphaeroides* oxidase (*15*, *46*−*48*) and the *Pseudomonas denitrificans* oxidase (*49*). Under most circumstances, these enzymes behave like the wild-type oxidases. The R481K mutation in the *R. sphaeroides* oxidase resulted in reductions in the midpoint potentials of heme *a* and heme a_3 of 40 and 15 mV, respectively. It was also deduced that the R481K mutation alters the pK_a of the heme a_3 D-propionate. This propionate is hydrogen bonded in the wild-type oxidase by R481 and also by W172, and the protonation state of this cluster appears to modulate the rate of internal electron transfer during catalytic turnover. The D-propionate cluster (including R481 and W172) has also been suggested to be the proton acceptor for pumped protons (*15*). Computational studies have also indicated that either the D-propionate of heme a_3 or R481 or W172 could function as the proton loading site proposed in the mechanism of the proton pump (*46*).

Computational approaches have also been used to examine a plausible mechanism for the transfer of a proton from E286 to the D-propionate of heme a_3 (*14*, *21*, *25*, *46*). There is a hydrophobic cavity that can accommodate water molecules between the presumed proton donor (E286) and the proton acceptor. These water molecules would provide a pathway for rapid proton transfer. Furthermore, the orientation of the water molecules between E286 and the D-propionate of heme a_3 has been computationally shown to depend on the charge distribution on the hemes. The water orientation within this cavity could act as a kinetic valve or gate, allowing pumped protons to exit but not to leak backward (*14*). Conformational changes of W172 and/or the collapse and formation of the water chain between E286 and the D-propionate of heme a_3 have also been suggested as mechanisms for gating the proton pump (*46*). The dynamics of the R481/D-propionate ion pair has been examined using molecular dynamics methods, and the movement of these residues is proposed to be a key factor in the water-mediated transfer of pumped protons as well as the transport of water out of the enzyme (*11*). In addition, such dynamics could also regulate the pK_a values of the D-propionates of both heme *a* and heme a_3 (*47*).

The equivalents of both the R481K (*49*) and W172F (*13*) mutants (R473K and W164F, respectively) have been characterized in the oxidase from *P. denitrificans*. The R481K mutant perturbs the FTIR reduced-minus-oxidized difference spectrum, and this was used to help assign the FTIR bands of the different heme propionates. Behr et al. (*49*) concluded that the D-propionate of heme *a*, but not that of heme a_3, is protonated upon reduction of the enzyme and, by extension, proposed to be protonated and deprotonated during the catalytic cycle.

The W164F mutant of the oxidase from *P. denitrificans* (equivalent to W172 in *R. sphaeroides*) retains 40% of the steady-state oxidase activity and has a reduced level of proton pumping (0.5 proton per electron) (*13*). In single-turnover (flow-flash) experiments, the W164F mutation appears to result in a delay in reprotonation of E286 (E278 in *P. denitrificans*) after the glutamate has donated its proton to the active site forming the P_R state, thus slowing the $P_R \rightarrow F$ transition. The FTIR spectra of the W164F mutant indicate perturbation of the heme propionates. In addition, the midpoint potential of heme a_3 is decreased by ~50 mV by the W164F mutation.

Our work confirms that R481 is important for the optimal function of cytochrome *c* oxidase. Even the replacement of this residue with a lysine lowers the midpoint potential of both hemes, although both oxidase activity and proton pumping remain unaltered (*47*). The R481H mutant results in a lower oxidase activity (18%), and the stoichiometry of the proton pump is approximately half that of the wild type. This is somewhat similar to the phenotype reported for the W164F oxidase of *P. denitrificans*. Proton pumping is not abolished; instead, the stoichiometry is reduced.

The less conservative mutations of the *R. sphaeroide*s enzyme examined in this work, R481N, R481Q, and R481L, all reduce the rate of oxidase turnover to ~5% of that of the wild type. Inhibition of steps in the reaction of the reduced enzyme with O_2 accounts for the reduced turnover rate. For the R481H mutant, the mutation appears to selectively lower the rate of the last step in the reaction sequence, the $F \rightarrow O$ transition. Since the previous step, $P_R \rightarrow F$, is due to the transfer of a proton from E286 to the active site, we conclude that this proton transfer is not altered by the R481H mutation. Possibly, the slower rate of the $F \rightarrow O$ step is due to a change in the electrochemical properties of the hemes, though this is pure speculation. The R481Q mutant clearly inhibits the rate of transfer of an electron from heme *a* to the binuclear center, measured by the $A \rightarrow P_R$ transition. More drastic, however, is the inhibition of steps following the formation of the P_R state ($P_R \rightarrow F$ and $F \rightarrow O$), suggesting the transfer of a proton from E286 is also influenced by the mutation. This is also observed for the W164F mutant of the oxidase from *P. denitrificans*, where the $P_R \rightarrow F$ step is also inhibited (*49*).

The most perturbed structural variant examined in this work was the R481L mutant oxidase. Its oxidase activity is similar to that of R481Q (~5%), but the flow-flash single-turnover study indicates that even the initial formation of the O_2 complex is delayed compared to that of the wild type. This suggests some conformational alteration limiting access to the active site by O_2 diffusing from the external medium. Once the initial complex with the fully reduced enzyme and O_2 is formed, each electron and proton transfer step leading to the fully oxidized enzyme is strongly inhibited.

Electrochemical titrations of the wild-type and R481L mutant oxidases were performed (Figure 3). Results for the wild type were qualitatively similar to results reported for the oxidase from *P. denitrificans*, showing two waves corresponding to the oxidation of the interacting hemes (*41*). The midpoints of the two waves were shifted lower for the R481L mutant by 33 and 58 mV,

respectively. These values do not represent the midpoint potentials of heme *a* and heme a_3, since both hemes are represented in each wave, and a specific model would be required to obtain further details. Furthermore, the shapes of the titration curves of the mutant indicate that complete equilibration was not achieved over the entire redox range. For the purposes of this work, the observation that the R481L mutant results in lower midpoint potentials of the hemes is sufficient and is qualitatively similar to what has been reported for the R481K mutant of the *R. sphaeroides* oxidase (*47*) and the W164F mutant of the *P. denitrificans* oxidase (*13*). Each of these residues forms a hydrogen bond to the D-propionate of heme a_3.

Remarkably, despite the evidence of alterations of each step in the oxidation of the *R. sphaeroides* oxidase by the R481L mutation (Figure 5 and Table 3), the enzyme still functions as a proton pump, albeit with approximately half the stoichiometry of the wild type. The slow rate of binding by O_2 ($R \rightarrow A$), slow electron transfer ($A \rightarrow P_R$), slow proton transfer ($P_R \rightarrow F$), and slow coupled electron/proton transfer ($F \rightarrow O$) exhibited by this mutant do not completely disable the proton pump. It is, therefore, difficult to imagine that the dynamics of the R481/D-propionate ion pair plays a critical role in the mechanism of proton pumping. Similarly, it is also very unlikely that any member of the cluster containing R481, R482, the D-propionate of heme a_3, and W172 is the proton loading site, essential for the proton pump to function. Replacing R481 with a leucine should have a major influence on the pK_a values of all of these residues.

It is still quite likely, and seemingly unavoidable, that pumped protons must be transferred from E286 through the region of the protein occupied by R481 and the D-propionate of heme a_3. In the wild type, this might well involve waters hydrogen bonded to any or all of the residues in this cluster. Such pathways must also exist in the R481L mutant. The driving force for the pumped proton, however, must be provided by formation of a strong proton binding site outside of the cluster represented by R481, R482, W172, and the D-propionate of heme a_3. The best candidates for the proton loading site that remain are the A-propionate of heme a_3 and one of the histidine ligands to Cu_B.

REFERENCES

1. Ramirez, B. E., Malmstrom, B. G., Winkler, J. R., and Gray, H. B. (1995) The currents of life: The terminal electron-transfer complex of respiration. *Proc. Natl. Acad. Sci. U.S.A. 92*, 11949–11951.
2. Ferguson-Miller, S., and Babcock, G. T. (1996) Heme/Copper Terminal Oxidases. *Chem. Rev. 96*, 2889–2907.
3. Wikström, M. (2004) Cytochrome c Oxidase: 25 Years of the Elusive Proton Pump. *Biochim. Biophys. Acta 1655*, 241–247.
4. Brzezinski, P., and Gennis, R. B. (2008) Cytochrome c oxidase: Exciting progress and remaining mysteries. *J. Bioenerg. Biomembr. 40*, 521–531.
5. Branden, G., Gennis, R. B., and Brzezinski, P. (2006) Transmembrane proton translocation by cytochrome c oxidase. *Biochim. Biophys. Acta 1757*, 1052–1063.
6. Brzezinski, P. (2004) Redox-driven Membrane-bound Proton Pumps. *Trends Biochem. Sci. 29*, 380–387.
7. Gennis, R. B. (2004) Coupled Proton and Electron Transfer Reactions in Cytochrome Oxidase. *Front. Biosci. 9*, 581–591.
8. Brzezinski, P., and Adelroth, P. (2006) Design principles of proton-pumping haem-copper oxidases. *Curr. Opin. Struct. Biol. 16*, 465–472.
9. Belevich, I., Verkhovsky, M. I., and Wikström, M. (2006) Proton-coupled electron transfer drives the proton pump of cytochrome c oxidase. *Nature 440*, 829–832.
10. Hosler, J. P., Ferguson-Miller, S., and Mills, D. A. (2006) Energy transduction: Proton transfer through the respiratory complexes. *Annu. Rev. Biochem. 75*, 165–187.
11. Wikström, M., Ribacka, C., Molin, M., Laakkonen, L., Verkhovsky, M. I., and Puustinen, A. (2005) Gating of Proton and Water Transfer in the Respiratory Enzyme Cytochrome c Oxidase. *Proc. Natl. Acad. Sci. U.S.A. 102*, 10478–10481.
12. Puustinen, A., and Wikström, M. (1999) Proton Exit from the Heme-copper Oxidase of *Escherichia coli*. *Proc. Natl. Acad. Sci. U.S.A. 96*, 35–37.
13. Ribacka, C., Verkhovsky, M. I., Belevich, I., Bloch, D. A., Puustinen, A., and Wikström, M. (2005) An Elementary Reaction Step of the Proton Pump is Revealed by Mutation of Tryptophan-164 to Phenylalanine in Cytochrome c Oxidase from *Paracoccus denitrificans*. *Biochemistry 44*, 16502–16512.
14. Wikström, M., Verkhovsky, M. I., and Hummer, G. (2003) Water-gated Mechanism of Proton Translocation by Cytochrome c Oxidase. *Biochim. Biophys. Acta 1604*, 61–65.
15. Brädén, G., Brädén, M., Schmidt, B., Mills, D. A., Ferguson-Miller, S., and Brzezinski, P. (2005) The Protonation State of a Heme Propionate Controls ElectronTransfer in Cytochrome c Oxidase. *Biochemistry 44*, 10466–10474.
16. Pawate, A. S., Morgan, J., Namslauer, A., Mills, D. A., Brzezinski, P., Ferguson-Miller, S., and Gennis, R. B. (2002) A Mutation in Subunit I of Cytochrome Oxidase from *Rhodobacter sphaeroides* Results in an Increase in Steady-State Activity But Completely Eliminates Proton Pumping. *Biochemistry 41*, 13417–13423.
17. Namslauer, A., Pawate, A., Gennis, R. B., and Brzezinski, P. (2003) Redox-Coupled Proton Translocation in Biological Systems: Proton Shuttling in Cytochrome c Oxidase. *Proc. Natl. Acad. Sci. U.S.A. 100*, 15543–15547.
18. Brändén, G., Pawate, A. S., Gennis, R. B., and Brzezinski, P. (2006) Controlled Uncoupling and Recoupling of Proton Pumping in Cytochrome c Oxidase. *Proc. Natl. Acad. Sci. U.S.A. 103*, 317–322.
19. Wikstrom, M., and Verkhovsky, M. I. (2007) Mechanism and energetics of proton translocation by the respiratory heme-copper oxidases. *Biochim. Biophys. Acta 1767*, 1200–1214.
20. Iwata, S., Ostermeier, C., Ludwig, B., and Michel, H. (1995) Structure at 2.8 Å Resolution of Cytochrome c Oxidase from *Paracoccus denitrificans*. *Nature 376*, 660–669.
21. Hofacker, I., and Schulten, K. (1998) Oxygen and Proton Pathways in Cytochrome c Oxidase. *Proteins 30*, 100–107.
22. Qian, J., Shi, W., Pressler, M., Hoganson, C., Mills, D., Babcock, G. T., and Ferguson-Miller, S. (1997) Aspartate-407 in *Rhodobacter sphaeroides* Cytochrome c Oxidase is not Required for Proton Pumping or Manganese Binding. *Biochemistry 36*, 2539–2543.
23. Tsukihara, T., Shimokata, K., Katayama, Y., SHimada, H., Muramoto, K., Aoyama, H., Mochizuki, M., Shinzawa-Itoh, K., Yamashita, E., Yao, M., Ishimura, Y., and Yoshikawa, S. (2003) The Low-Spin Heme of Cytochrome c Oxidase as the Driving Element of the Proton-Pumping Process. *Proc. Natl. Acad. Sci. U.S.A. 100*, 15304–15309.
24. Popovic, D. M., and Stuchebrukhov, A. A. (2005) Proton Exit Channels in Bovine Cytochrome c Oxidase. *J. Phys. Chem. B 109*, 1999–2006.
25. Zheng, X., Medvedev, D. M., Swanson, J., and Stuchebrukhov, A. A. (2003) Computer Simulation of Water in Cytochrome c Oxidase. *Biochim. Biophys. Acta 1557*, 99–107.
26. Quenneville, J., Popovic, D. M., and Stuchebrukhov, A. A. (2006) Combined DFT and electrostatics study of the proton pumping mechanism in cytochrome c oxidase. *Biochim. Biophys. Acta 1757*, 1035–1046.
27. Mills, D. A., Xu, S., Geren, L., Hiser, C., Qin, L., Sharpe, M. A., McCracken, J., Durham, B., Millett, F., and Ferguson-Miller, S. (2008) Proton-dependent electron transfer from Cu_A to heme a and altered EPR spectra in mutants close to heme a of cytochrome oxidase. *Biochemistry 47*, 11499–11509.
28. Siegbahn, P. E. M., and Blomberg, M. R. A. (2008) Proton Pumping Mechanism in Cytochrome c Oxidase. *J. Phys. Chem. A 112*, 12772–12780.
29. Siegbahn, P. E., and Blomberg, M. R. (2007) Energy diagrams and mechanism for proton pumping in cytochrome c oxidase. *Biochim. Biophys. Acta 1767*, 1143–1156.
30. Sugitani, R., Medvedev, E. S., and Stuchebrukhov, A. A. (2008) Theoretical and computational analysis of the membrane potential generated by cytochrome c oxidase upon single electron injection into the enzyme. *Biochim. Biophys. Acta 1777*, 1129–1139.
31. Michel, H. (1999) Cytochrome c Oxidase: Catalytic Cycle and Mechanisms of Proton Pumping—A Discussion. *Biochemistry 38*, 15129–15140.
32. Fee, J. A., Case, D. A., and Noodleman, L. (2008) Toward a chemical mechanism of proton pumping by the B-type cytochrome c oxidases: Application of density functional theory to cytochrome ba_3 of *Thermus thermophilus*. *J. Am. Chem. Soc. 130*, 15002–15021.

33. Sharpe, M. A., and Ferguson-Miller, S. (2008) A chemically explicit model for the mechanism of proton pumping in heme-copper oxidases. *J. Bioenerg. Biomembr. 40*, 541–549.
34. Das, T. K., Gomes, C. M., Teixeira, M., and Rousseau, D. L. (1999) Redox-linked Transient Deprotonation at the Binuclear Site in the aa_3-type Quinol Oxidase from *Acidianus ambivalens*: Implications for Proton Translocation. *Proc. Natl. Acad. Sci. U.S.A. 96*, 9591–9596.
35. Yoshikawa, S., Muramoto, K., Shinzawa-Itoh, K., Aoyama, H., Tsukihara, T., Ogura, T., Shimokata, K., Katayama, Y., and Shimada, H. (2006) Reaction mechanism of bovine heart cytochrome c oxidase. *Biochim. Biophys. Acta 1757*, 395–400.
36. Kawasaki, M., Mogi, T., and Anraku, Y. (1997) Substitutions of Charged Amino Acid Residues Conserved in Subunit I Perturb the Redox Metal Centers of the *Escherichia coli* bo-type Ubiquinol Oxidase. *J. Biochem. 122*, 422–429.
37. Mitchell, D. M., and Gennis, R. B. (1995) Rapid Purification of Wildtype and Mutant Cytochrome c Oxidase from *Rhodobacter sphaeroides* by Ni^{2+}-NTA Affinity Chromatography. *FEBS Lett. 368*, 148–150.
38. Keen, N. T., Tamaki, S., Kobayashi, D., and Trollinger, D. (1988) Improved Broad-Host-Range Plasmids for DNA Cloning in Gram-Negative Bacteria. *Gene 70*, 191–197.
39. Hiser, C., Mills, D. A., Schall, M., and Ferguson-Miller, S. (2001) C-Terminal Truncation and Histidine-tagging of Cytochrome c Oxidase Subunit II Reveals the Native Processing Site, Shows Involvement of the C-terminus in Cytochrome c Binding, and Improves the Assay for Proton Pumping. *Biochemistry 40*, 1606–1615.
40. Verkhovsky, M. I., Morgan, J. E., and Wikström, M. (1995) Control of Electron Delivery to the Oxygen Reduction Site of Cytochrome c Oxidase: A Role for Protons. *Biochemistry 34*, 7483–7491.
41. Gorbikova, E. A., Vuorilehto, K., Wikstrom, M., and Verkhovsky, M. I. (2006) Redox Titration of all Electron Carriers of Cytochrome c Oxidase by Fourier Transform Infrared Spectroscopy. *Biochemistry 45*, 5641–5649.
42. Blair, D. F., Ellis, J., Walther, R., Wang, H., Gray, H. B., and Chan, S. I. (1986) Spectroelectrochemical Study of Cytochrome c Oxidase: pH and Temperature Dependences of the Cytochrome Potentials. *J. Biol. Chem. 261*, 11524–11537.
43. Adelroth, P., Ek, M., and Brzezinski, P. (1998) Factors Determining Electron-Transfer Rates in Cytochrome c Oxidase: Investigation of the Oxygen Reaction in the *R. sphaeroides* Enzymes. *Biochim. Biophys. Acta 1367*, 107–117.
44. Verkhovsky, M. I., Morgan, J. E., Verkhovskaya, M. L., and Wikström, M. (1997) Translocation of Electrical Charge During a Single Turnover of Cytochrome c Oxidase. *Biochim. Biophys. Acta 1318*, 6–10.
45. Faxén, K., Gilderson, G., Adelroth, P., and Brzenzinski, P. (2005) A Mechanistic Principle for Proton Pumping by Cytochrome c Oxidase. *Nature 437*, 286–289.
46. Seibold, S. A., Mills, D. A., Ferguson-Miller, S., and Cukier, R. I. (2005) Water Chain Formation and Possible Proton Pumping Routes in *Rhodobacter sphaeroides* Cytochrome c Oxidase: A Molecular Dynamics Comparison of the Wild Type and R481K Mutant. *Biochemistry 44*, 10475–10485.
47. Mills, D. A., Geren, L., Hiser, C., Schmidt, B., Durham, B., Millett, F., and Ferguson-Miller, S. (2005) An Arginine to Lysine Mutation in the Vicinity of the Heme Propionates Affects the Redox Potentials of the Hemes and Associated Electron and Proton Transfer in Cytochrome c Oxidase. *Biochemistry 44*, 10457–10465.
48. Qian, J., Mills, D. A., Geren, L., Wang, K., Hoganson, C. W., Schmidt, B., Hiser, C., Babcock, G. T., Durham, B., Millett, F., and Ferguson-Miller, S. (2004) Role of the Conserved Arginine Pair in Proton and Electron Transfer in Cytochrome c Oxidase. *Biochemistry 43*, 5748–5756.
49. Behr, J., Michel, H., Mäntele, W., and Hellwig, P. (2000) Functional Properties of the Heme Propionates in Cytochrome c Oxidase from *Paracoccus denitrificans*. Evidence from FTIR Difference Spectroscopy and Site-Directed Mutagenesis. *Biochemistry 39*, 1356–1363.